Boride Magnets Hot Paper

DOI: 10.1002/anie.201406397

Unexpected Synergy between Magnetic Iron Chains and Stacked B_6 Rings in $Nb_6Fe_{1-x}Ir_{6+x}B_8$**

*Mohammed Mbarki, Rachid St. Touzani, and Boniface P. T. Fokwa**

Abstract: *The synergistic combination of experiment and density functional theory has led to the discovery of the first ferromagnetic material, $Nb_6Fe_{1-x}Ir_{6+x}B_8$, containing in its crystal structure iron chains embedded in stacked B_6 rings. The strong ferromagnetic Fe–Fe interactions found in the iron chains induce an unexpected strengthening of the B–B interactions in the B_6 rings. Beside these strong B–B interactions, strong interlayer metal–boron bonds (Ir–B and Nb–B) ensure the overall structural stability of this phase, while the magnetic Fe–Fe interactions are mainly responsible for the observed ferromagnetic ordering below $T_C = 350$ K.*

The use of planar boron rings as building blocks for designing new solid-state materials has been predicted by experimentalists and theoreticians studying gas-phase species.[1–4] One of these rings, namely the planar B_6 ring was discovered recently in the solid-state phase $Ti_7Rh_4Ir_2B_8$, whose crystal structure contains titanium atoms sandwiched between B_6 rings.[5] Recently, isolated TaB_6Ta species could be found in the gas phase, indicating the ability of this planar B_6 ring to strongly bind to transition metals, even in the gas phase.[6]

A challenge for functional materials design is the use of such a strongly binding boron entity to make new solid-state phases with interesting physical properties. As alluded to in the publication on $Ti_7Rh_4Ir_2B_8$, the presence of titanium chains in its crystal structure indicates the possibility to build chains of 3d magnetically active elements in solid-state compounds containing B_6 rings.[5] Such chains have been extensively studied, both theoretically and experimentally. It was predicted that an infinite unsupported linear chain with short-range magnetic interactions will not have long-range magnetic order at a finite temperature.[7] However, when interacting with a substrate (for example Co chains on Pt substrate) that supports the one-dimensional nanostructures, long-range ferromagnetic order emerges.[8] In the bulk, such chains of magnetically active elements, well separated from each other, have also been the subject of theoretical and experimental investigations in recent years.[9–13] In particular, the $Ti_3Co_5B_2$ structure type has produced phases with a wide spectrum of long-range magnetic order, for example antiferromagetism in $Mg_2MnRh_5B_2$ or ferromagnetism in $Sc_2CoIr_5B_2$.[13] Furthermore, drastic variation of the magnetic properties has been reported recently in the compound series $Sc_2FeRu_{5-n}Rh_nB_2$, $Ti_2FeRu_{5-n}Rh_nB_2$, and $Sc_2FeRu_{5-n}Ir_nB_2$ ($n = 0$–5), thereby indicating the crucial role of magnetically inactive 4d and 5d transition metals on the magnetic properties of these rare-earth-free itinerant magnetic materials.[9–11] In the crystal structure of these phases, boron atoms are isolated from each other and they do not interact with the 3d transition metals (including the magnetically active element) too. A different situation is found in the recently discovered $Ti_7Rh_4Ir_2B_8$ and $M_7T_6B_8$ (M = Nb, Ta; T = Ru, Rh, Ir) phases,[14] in which the titanium, niobium, and tantalum chains strongly interact with the B_6 rings. Therefore, inducing long-range magnetic order in these phases, by substituting non-magnetic chains by chains of magnetically active elements is not granted, because of the possible strong bonding interactions of these magnetic chains with the B_6 rings.

Herein, we report experimental and theoretical investigations of the first solid-state phase, whose crystal structure contains chains of a magnetically active element (iron) interacting with B_6 rings.

Our experimental and theoretical investigations were carried out at the same time and both were based on the idea of replacing chains of titanium, niobium, or tantalum atoms by chains of iron atoms in the respective crystal structures. The linking of the two methods turns out to be the key for a successful substitution of one niobium by iron in $Nb_7Ir_6B_8$ on the way to $Nb_6FeIr_6B_8$ (see Figure 1) starting, however, from the elements to achieve the expected phase and structure.

The calculated reaction enthalpy indicates a favorable product by about 1036 kJ mol^{-1}, which is not far from the 1249 kJ mol^{-1} obtained for the ternary $Nb_7Ir_6B_8$ phase. These results indicate also that the ternary phase should be thermodynamically more stable than the quaternary, which was further confirmed by a calculated reaction enthalpy between the two phases, which favors the ternary by 44 kJ mol^{-1}. Of all ternary $M_7T_6B_8$ phases, those with T = Ir have been reported to be difficult to synthesize and no single crystals could be obtained.[14] Consequently, the thermodynamically less-stable quaternary Ir-based phase should be even more difficult to synthesize under the same conditions. Indeed, only about 12 % of the expected phase was obtained when applying the same synthetic procedure reported for the ternary phase. However, after arc melting for just a few

[*] Dipl.-Chem. M. Mbarki,[+] M.Sc. R. St. Touzani,[+]
Priv.-Doz. Dr. B. P. T. Fokwa
Institute of Inorganic Chemistry, RWTH Aachen University
Landoltweg 1, 52056 Aachen (Germany)
E-mail: boniface.fokwa@ac.rwth-aachen.de
Homepage: http://www.ssc.rwth-aachen.de/fokwa

[+] These authors contributed equally to this work.

[**] We thank Deutsche Forschungsgemeinschaft for financial support (Heisenberg fellowship to B.P.T. Fokwa), Resi Zaunbrecher (IPC, RWTH Aachen) and Daniel Grüner (FZ Jülich) for the EDX and metallographic analyses as well as Christina Houben (IAC, RWTH Aachen) and Dr. Yinguo Xiao (FZ Jülich) and Prof. Olivier Isnard (CNRS Grenoble) for the magnetic measurements.

Supporting information for this article is available on the WWW under http://dx.doi.org/10.1002/anie.201406397.

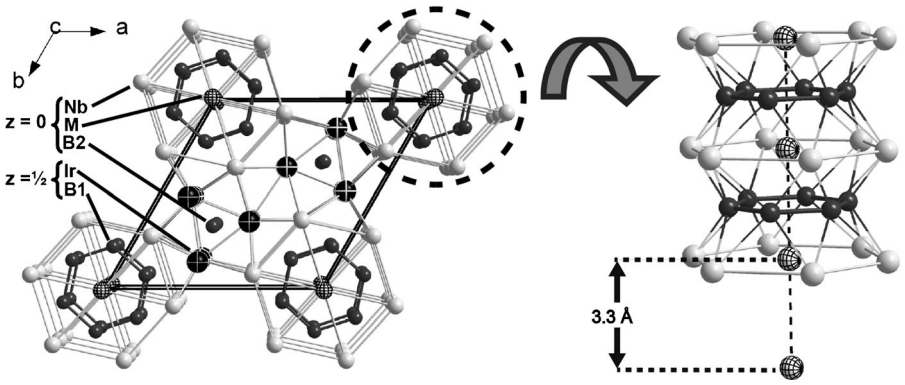

Figure 1. Projection of the crystal structure of $Nb_6MIr_6B_8$ ($M = Fe_{0.77(2)}Ir_{0.23(2)}$ in the experiment and M = Fe in theory) along [001]. The two different layers ($z = 0$ and $z = {}^1/_2$) are indicated. Part of the structure (right) showing M atoms sandwiched by B_6 rings and surrounded by Nb_6 rings. The intrachain M–M distance is indicated.

seconds the reaction product was analyzed and an unexpected and drastic increase of the amount of the phase (ca. 61%) resulted, and most importantly, high crystallinity and many single crystals were obtained. The fact that the amount of the expected phase increases after a far smaller reaction time (rapid quenching) suggests a kinetically stabilized phase. Rietveld refinements (see Supporting Information, Figure S1) of the X-ray powder data, metallographic and energy dispersive X-ray (EDX) spectroscopy analyses confirmed the synthesis of the expected phase together with the side phases $NbIr_{3-x}Fe_xB_y$ (ca. 31%, $x \approx 0.3$, $y \approx 0.05$, Cu_3Au-type) and NbB_2 (ca. 8%).[15] Furthermore, single-crystal refinement results (see Tables S1 and S2 in the Supporting Information) indicate, indeed, that iron is sandwiched between the B_6 rings in the structure, however, the Fe site could only be filled when mixed with about 23% of the electron-richer iridium (see Figure 1), leading to the chemical formula $Nb_6Fe_{0.77(2)}Ir_{6.23(2)}B_8$, in accordance with the presence of iron in the side phase.

The experimentally obtained lattice parameters ($a =$ 9.302(3) Å, $c = 3.3086(9)$ Å) are smaller than those of the ternary phase, as expected, but significantly different ($\Delta a = +$ 0.2 Å and $\Delta c = -0.1$ Å) to those calculated using the optimization procedure (GGA functional) for the ideal $Nb_6FeIr_6B_8$ composition within the VASP code on the non-magnetic (NM) structure. However, because magnetic ordering is possible owing to the presence of iron in the structure, two magnetic ordering models (ferromagnetic, FM, and antiferromagnetic, AFM, using a 2*c*-supercell with alternating parallel and antiparallel iron spins in the *c* direction) were studied theoretically. The effect of magnetic ordering was clear, as the new lattice parameters were closer to the experimental ones, and those of the energetically favorable FM model (-3.86 kJ mol^{-1} more stable than AFM and -31.84 kJ mol^{-1} more stable than NM) were now only $\Delta a = +0.1$ Å and $\Delta c = -0.03$ Å far from the experimental ones. This finding indicates that the synthesized phase will likely order ferromagnetically.

The electronic density of states (DOS) of the non-spin-polarized (non-magnetic) structure (Figure 2, left) has a high peak at the Fermi level (E_F) mainly originating from the iron 3d states. After spin polarization (ferromagnetic model) the peak disappears and E_F now lies in a pseudogap (Figure 2, right), indicating that iron alone is responsible for the predicted ferromagnetic ordering, in particular because the calculated atomic magnetic moments on Nb and Ir are negligible (on average 0.05 μ_B and 0.03 μ_B, respectively) if compared to that of Fe (2.64 μ_B). Furthermore, the DOS at E_F is non-zero, indicating metallic behavior and thus predicting the new phase to be an itinerant ferromagnet.

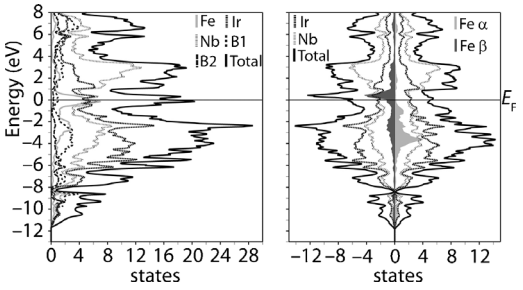

Figure 2. Total and projected DOS of non-spin-polarized (nsp) calculation (left) and spin-polarized (sp) calculation (right) for the hypothetical ferromagnetic $Nb_6FeIr_6B_8$ phase. All curves have been shifted so that the Fermi level lies at the energy zero. For Fe the α-spin density is light gray and β-spin density dark gray.

Thermomagnetic investigations (2–600 K) reveal, indeed, that the new phase orders ferromagnetically well above room temperature ($T_C = 350$ K, see the atomic magnetic dipole moment (μ_a) vs temperature (T) curve, Figure 3). The Curie temperature (T_C) is well below that of elemental cubic iron (α-Fe, $T_C = 1044$ K),[16] suggesting that α-Fe is not responsible for this magnetic ordering, in accordance with the absence of elemental iron in the analyzed product. The Curie–Weiss behavior, observed above the ordering temperature of the reciprocal susceptibility versus temperature plot (see Figure 3, insert), clearly indicates ferromagnetic interactions with a high and positive Weiss constant (+261 K). The magnetic hysteresis recorded at 5 K shows a coercivity in the range of semi-hard materials ($H_C = 8$ kA m^{-1}, see Figure S2 in the Supporting Information) but the hysteresis loop is not saturated at 5 T, reaching a magnetic moment of 1.2 μ_B. Because the hysteresis is not saturated, the value of the total magnetic moment is far below that calculated theoretically. Furthermore, single-crystal structure refinement revealed that the 1*a* iron site needs about 23% of the electron-richer iridium to be filled (see Figure 1), thereby significantly reducing the overall magnetic moment expected for a fully occupied iron site.

As mentioned above already, ferromagnetic Fe chains have proven to be excellent building units for achieving

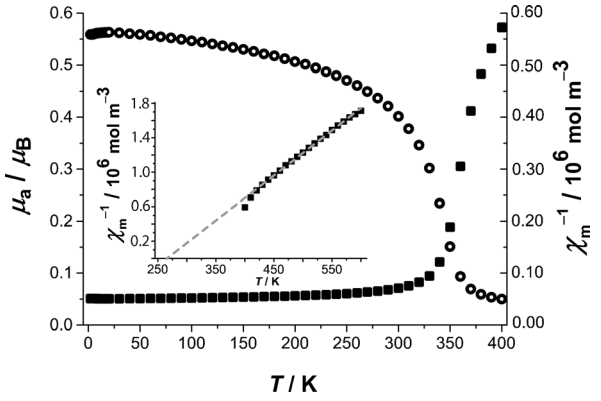

Figure 3. Magnetization and reciprocal susceptibility versus temperature at an applied field of 0.1 T for $Nb_6Fe_{0.77(2)}Ir_{6.23(2)}B_8$. Insert: reciprocal susceptibility versus temperature showing the Curie–Weiss behavior above 425 K. The dashed gray line indicates the Curie–Weiss straight line with a Weiss constant of +261 K.

itinerant magnetism in the solid state,[9–13] but the fact that each iron atom in the new structure is sandwiched between B_6 rings is new and therefore special attention should be devoted to this interaction. First, the new crystal structure is built up by two layers at $z = 0$ and $z = {}^1/_2$: The layer at $z = 0$ contains isolated boron atoms (B2) and the less-dense metals (Nb and Fe) while at $z = {}^1/_2$ the planar B_6 ring (B1) and the metal with the highest electron density (Ir) are found. Just like in the case of the isotypic $Ti_7Rh_4Ir_2B_8$, the bonding is really complex, and as demonstrated below, the layer description of the crystal structure is not completely followed by the bonding interactions. Chemical bonding analyses, based on the COHP method and its energy integral (ICOHP), were conducted for the ideal $Nb_6FeIr_6B_8$ composition in non-spin-polarized and spin polarized approaches, to analyze the influence of magnetism on the bonding situation. The results (see ICOHPs of Tables S3 and S4 as well as Figures S3 and S4 in the Supporting Information) indicate that the Nb–B1, Ir–B2, Nb–Nb, Nb–Ir, and Ir–Ir bonds are not affected by spin-polarization, in contrast to all the interactions at the nearby of iron atoms, Fe–Fe, Fe–B, B1–B1, and Nb–Fe. Before moving to the overall stability of the structure, let's first focus on the effect of magnetism on the bonding situation around iron. In the non-spin-polarized calculation the ICOHP values of Fe–Fe, Nb–Fe, Fe–B1, and B1–B1 bonds are −0.28, −0.76, −1.40, and −3.25 eV, respectively. After spin polarization two behaviors emerge: While the first three bonds get significantly weaker (smaller ICOHP values, −0.22, −0.61, −1.15 eV), only the B1–B1 interaction becomes stronger (larger ICOHP value, −3.34 eV). In fact, the strong ferromagnetic exchange interactions in the iron chains (see DOS analysis above) weakens all the weak bonds around iron and strengthens even more the already strong B1–B1 bonds in the B_6 rings (see Figure S3). In other words, less electron density on B1 is engaged in the building of bonds with iron, thereby leaving iron with more electron density which is necessary for magnetic interactions in the iron chains, while the excess electron density on B1 increases the bonding in the B_6 ring, thus achieving a great magneto-bonding synergy of this novel structural unit that is iron chains embedded between stacked B_6 rings.

To study the overall stability of the new structure, we have considered all the bonds in the unit cell to take into account not only the strength of an interaction but also its amount in the unit cell (see Table S3). Starting with the strongest B1–B1 bonds, of which there are six (B_6 ring) per unit cell, they all contribute about 9.4% of the overall unit-cell energy (ICOHP sum per cell). Note that the B1–B1 distance (1.84 Å) within the B_6 ring in this new phase is comparable to that found in other B_6-containing molecules and solid-state phases: for example, 1.70–1.78 Å in the triple-decker $[(Cp^*Re)_2B_6X_6]$ complex,[17] 1.79 Å in $Ti_7Rh_4Ir_2B_8$ and 1.74–1.96 Å in $M_7T_6B_8$ (M = Nb, Ta; T = Ru, Rh, Ir) phases. The second strongest bonds in the structure are the interlayer metal–boron bonds, of which those with Ir (Ir–B2) are approximately 0.6 eV stronger than those with Nb (Nb–B1) because much of the electron density on B1 is engaged in the building of the B6 ring in contrast to B2 which is isolated (no B2–B2 bond). These two types of heteroatomic interactions (36 in the unit cell) account for 38.6% of the total binding energy of the unit cell. However, intralayer metal–boron interactions (Ir–B1 and Nb–B2) also exist, but are significantly weaker (see Table S3) with ICOHP values in the range of the rather weak interlayer Fe–B1 interactions. Nevertheless, all these three interactions still contribute 13.6% of the total binding energy because of their large number (24) in the unit cell. Concerning the metal–metal interactions, the interlayer Nb–Ir contacts are also very strong, and contribute even more than the intralayer metal–boron contacts, as they account for 26.9% (for 36 bonds) of the total binding energy. The other metallic Ir–Ir, Nb–Nb, and Nb–Fe interactions (distance cutoff at 3.02 Å) are the weakest with a contribution of 11,3% for all 21 contacts. The Fe–Fe distance of 3.31 Å is too weak to be considered as bonding, however, the effect of spin polarization on the Fe–Fe interaction is huge; its non-spin-polarized curve shows a strong peak in the anti-bonding area at E_F, which is, however, removed after spin-polarization owing to the splitting in α- and β-COHP curves (Figure S4). This effect was not observed for the other Fe-containing interactions (Fe–B1 and Fe–Nb), indicating that the Fe–Fe interactions are mainly responsible for the observed ferromagnetic ordering in the new phase.

$Nb_6Fe_{1-x}Ir_{6+x}B_8$ is the first ferromagnetic solid-state compound containing in its crystal structure a chain of a magnetically active element (Fe) embedded between stacked B_6 rings. DFT calculations reveal a great synergy between Fe–Fe magnetic interactions within the iron chains and the B1–B1 bonding interactions in the B_6 rings. This finding should pave the way for new magnetic materials containing low-dimensional magnetic substructures (chains, ladders) interacting with planar B_n ($n > 3$) units.

Experimental Section

Powder samples and needle-shaped silvery single crystals of the title phase were synthesized in a few seconds by arc-melting high purity elements (at least 99.9%, starting ratio, Nb:Fe:Ir:B of 6:1:6:8) in a water-cooled copper crucible under an argon atmosphere. For

details concerning the synthetic steps see Ref. [9] Crystal data of $Nb_6Fe_{0.77(2)}Ir_{6.23(2)}B_8$: hexagonal, $a = 9.302(3)$, $c = 3.3086(9)$ Å, $V = 247.9(2)$ Å^3, $T = 293(2)$ K, space group $P6/m$ (no. 175) which is the highest space group found from the diffraction data, $Z = 1$; diffraction data collected on a Bruker SMART APEX CCD diffractometer with graphite-monochromatized Mo-K_α radiation ($\lambda = 0.71073$ Å), semi-empirical absorption correction with SADABS,[18a] 2002 reflections measured, 294 unique ($R_{int} = 0.0647$). The final values for R_1 and wR_2 (all data, 20 parameters) were 0.0420 and 0.0722, respectively. The crystal-structure solution and refinement were carried out by means of the SHELX programs.[18b] (See Table S1). Further details on the crystal structure investigations may be obtained from the Fachinformationszentrum Karlsruhe, 76344 Eggenstein-Leopoldshafen, Germany (fax: (+49) 7247-808-666; e-mail: crysdata@fiz-karlsruhe.de), on quoting the depository number CSD-427883). The crystallographic data collected for several single crystals provided identical chemical compositions and the presence of all metals was confirmed by EDX analysis on several crystals. No superstructure reflections could be found even at 100 K. Metallographic analyses were carried out on a bulk compact sample prepared using the standard metallographic procedure and analyzed on a high-resolution REM of the type Zeiss SUPRA 50 VP (Zeiss, Oberkochen, Germany) equipped with an EDX system of the type INCA (Oxford, England). The sample was sputtered with a 2 nm-thick platinum layer. The magnetic measurements were conducted on polycrystalline samples by using a SQUID magnetometer (MPMS-5S, Quantum Design) in the temperature range 2.0–400 K and a Physical Properties Measurement System (PPMS, Quantum Design, San Diego, USA) for 300–600 K under an external field of 0.1 T. Hysteresis loops were measured between −5 and +5 T at 5 K. Details concerning sample arrangement and measurement technique are described elsewhere.[19] The data were corrected for the sample holder (Teflon tubes). $NbIr_{3-x}Fe_x$ was resynthesized and checked for any magnetic ordering, but only paramagnetic behavior was found in the above mentioned experimental conditions, indicating that the magnetic ordering is due to the main phase only.

All electronic-structure calculations were based on density functional theory using plane wave basis sets[20a] as incorporated in the VASP suite (for structure optimization)[20b] using the exchange correlation functional GGA (generalized gradient approximation) as parameterized by Perdew, Burke, and Ernzerhof,[20c] and the algorithm by Monkhorst and Pack.[20d] For the calculation of the density-of-states the scalar-relativistic Linear Muffin-Tin Orbital Atomic Spheres Approximation (LMTO-ASA) theory[21a,b] was used, in its tight-binding representation[21c] using the TB-LMTO-ASA 4.7 code[21d] with the GGA functional parameterized by Perdew and Wang.[21e] Bonding analysis was performed by the Crystal Orbital Hamilton Population (COHP) technique[21f] as implemented in TB-LMTO-ASA 4.7. For details concerning the calculation steps see, for example, Ref. [22].

Received: June 19, 2014
Published online: August 21, 2014

Keywords: boron rings · iron · magnetic properties · solid-state chemistry · stacking interactions

[1] A. N. Alexandrova, A. I. Boldyrev, H. J. Zhai, L. S. Wang, *Coord. Chem. Rev.* **2006**, *250*, 2811 – 2866.

[2] a) A. N. Alexandrova, A. I. Boldyrev, H. J. Zhai, L. S. Wang, E. Steiner, P. W. Fowler, *J. Phys. Chem. A* **2003**, *107*, 1359 – 1369; b) H. J. Zhai, A. N. Alexandrova, K. A. Birch, A. I. Boldyrev, L. S. Wang, *Angew. Chem.* **2003**, *115*, 6186 – 6190; *Angew. Chem. Int. Ed.* **2003**, *42*, 6004 – 6008.

[3] W. Huang, A. P. Sergeeva, H. J. Zhai, B. B. Averkiev, L. S. Wang, A. I. Boldyrev, *Nat. Chem.* **2010**, *2*, 202 – 206.

[4] E. Oger, N. R. M. Crawford, R. Kelting, P. Weis, M. M. Kappes, R. Ahlrichs, *Angew. Chem.* **2007**, *119*, 8656 – 8659; *Angew. Chem. Int. Ed.* **2007**, *46*, 8503 – 8506.

[5] B. P. T. Fokwa, M. Hermus, *Angew. Chem.* **2012**, *124*, 1734 – 1737; *Angew. Chem. Int. Ed.* **2012**, *51*, 1702 – 1705.

[6] W. L. Li, L. Xie, T. Jian, C. Romanescu, L.-S. Wang, *Angew. Chem.* **2014**, *126*, 1312 – 1316; *Angew. Chem. Int. Ed.* **2014**, *53*, 1288 – 1292.

[7] a) L. D. Landau, E. M. Lifshitz, *Stat. Phys.* **1959**, *5*, 482; b) E. Ising, *Z. Phys.* **1925**, *31*, 253 – 258; c) N. D. Mermin, H. Wagner, *Phys. Rev. Lett.* **1966**, *17*, 1133 – 1136.

[8] P. Gambardella, A. Dallmeyer, K. Maiti, M. C. Malagoli, W. Eberhardt, K. Kern, C. Carbone, *Nature* **2002**, *416*, 301 – 304.

[9] M. Hermus, M. Yang, D. Grüner, F. J. DiSalvo, B. P. T. Fokwa, *Chem. Mater.* **2014**, *26*, 1967 – 1974.

[10] B. P. T. Fokwa, H. Lueken, R. Dronskowski, *Eur. J. Inorg. Chem.* **2011**, 3926.

[11] a) B. P. T. Fokwa, *Eur. J. Inorg. Chem.* **2010**, 3075 – 3092; b) "Borides, Solid-State Chemistry": B. P. T. Fokwa in *Encyclopedia of Inorganic and Bioinorganic Chemistry* (Ed.: R. A. Scott), Wiley, **2014**, DOI: 10.1002/9781119951438.eibc0022.-pub2.

[12] a) B. P. T. Fokwa, H. Lueken, R. Dronskowski, *Chem. Eur. J.* **2007**, *13*, 6040 – 6046; b) G. D. Samolyuk, B. P. T. Fokwa, R. Dronskowski, G. J. Miller, *Phys. Rev. B* **2007**, *76*, 094404.

[13] a) E. A. Nagelschmitz, W. Jung, *Chem. Mater.* **1998**, *10*, 3189 – 3195; b) E. A. Nagelschmitz, W. Jung, R. Feiten, P. Müller, H. Lueken, *Z. Anorg. Allg. Chem.* **2001**, *627*, 523 – 532; c) R. Dronskowski, K. Korczak, H. Lueken, W. Jung, *Angew. Chem.* **2002**, *114*, 2638 – 2642; *Angew. Chem. Int. Ed.* **2002**, *41*, 2528 – 2532.

[14] Q. Zheng, M. Kohout, R. Gumeniuk, N. Abramchuk, H. Borrmann, Y. Prots, U. Burkhardt, W. Schnelle, L. Akselrud, H. Gu, A. Leithe-Jasper, Y. Grin, *Inorg. Chem.* **2012**, *51*, 7472.

[15] FindIt, Inorganic Crystal Structure Database, Version 1.9.3, FIZ Karlsruhe, 2013 – 2.

[16] H. Lueken, Magnetochemie, Teubner, Stuttgart, **1999**.

[17] B. Le Guennic, H. Jiao, S. Kahlal, J.-Y. Saillard, J.-F. Halet, S. Ghosh, M. Shang, A. M. Beatty, A. L. Rheingold, T. P. Fehlner, *J. Am. Chem. Soc.* **2004**, *126*, 3203.

[18] a) G. M. Sheldrick, SADABS, University of Göttingen (Germany), **2001**; b) G. M. Sheldrick, *Acta Crystallogr. Sect. A* **2008**, *64*, 112 – 122.

[19] S. Hatscher, H. Schilder, H. Lueken, W. Urland, *Pure Appl. Chem.* **2005**, *77*, 497 – 511.

[20] a) P. E. Blöchl, *Phys. Rev. B* **1994**, *50*, 17953; b) G. Kresse, D. Joubert, *Phys. Rev.* **1999**, *59*, 1758 – 1775; c) J. P. Perdew, K. Burke, M. Ernzerhof, *Phys. Rev. Lett.* **1996**, *77*, 3865 – 3868; d) H. J. Monkhorst, J. D. Pack, *Phys. Rev. B* **1976**, *13*, 5188 – 5192.

[21] a) O. K. Andersen, *Phys. Rev. B* **1975**, *12*, 3060 – 3083; b) O. K. Andersen, H. Skriver, H. Nohl, B. Johansson, *Pure Appl. Chem.* **1980**, *52*, 93 – 118; c) O. K. Andersen, O. Jepsen, *Phys. Rev. Lett.* **1984**, *53*, 2571 – 2574; d) O. K. Andersen, R. W. Tank, O. Jepsen, TB-LMTO-ASA v. 4.7, Max-Planck-Institut für Festkörperforschung Stuttgart, **1998**; e) J. P. Perdew, Y. Wang, *Phys. Rev. B* **1992**, *45*, 13244; f) R. Dronskowski, P. E. Blöchl, *J. Phys. Chem.* **1993**, *97*, 8617 – 8624.

[22] R. St. Touzani, B. P. T. Fokwa, *J. Solid State Chem.* **2014**, *211*, 227 – 234.

